

Hamming OCR: A Locality Sensitive Hashing Neural Network for Scene Text Recognition

Bingcong Li*, Xin Tang*, Xianbiao Qi*, Yihao Chen, Rong Xiao

Visual Computing Group, Ping An Property & Casualty Insurance
libingcong894@pingan.com.cn, {tangxint, qixianbiao, xiaorong}@gmail.com, o0o@o0oo0o.cc

Abstract

Recently, inspired by Transformer, self-attention-based scene text recognition approaches have achieved outstanding performance. However, we find that the size of model expands rapidly with the lexicon increasing. Specifically, the number of parameters for softmax classification layer and output embedding layer are proportional to the vocabulary size. It hinders the development of a lightweight text recognition model especially applied for Chinese and multiple languages. Thus, we propose a lightweight scene text recognition model named *Hamming OCR*. In this model, a novel Hamming classifier, which adopts locality sensitive hashing (LSH) algorithm to encode each character, is proposed to replace the softmax regression and the generated LSH code is directly employed to replace the output embedding. We also present a simplified transformer decoder to reduce the number of parameters by removing the feed-forward network and using cross-layer parameter sharing technique.

Compared with traditional methods, the number of parameters in both classification and embedding layers is independent on the size of vocabulary, which significantly reduces the storage requirement without loss of accuracy. Experimental results on several datasets, including four public benchmarks and a Chinese text dataset synthesized by SynthText¹ with more than 20,000 characters, shows that Hamming OCR achieves competitive results.

Introduction

Scene text recognition (Shi et al. 2016; Shi, Bai, and Yao 2016; Cheng et al. 2017; Li et al. 2019; Lu et al. 2019; Chen et al. 2020), which aims at extracting text content from images, has attracted enormous attention from both the academy and industry due to its great commercial value in various real-world applications.

With the development of sequence modeling, many text recognition models (Liu et al. 2016; Cheng et al. 2018; Liu, Chen, and Wong 2018) have achieved remarkable results. Generally, most competitive text recognition models have an encoder-decoder architecture, which maps each input sequence into an output sequence of variable length. Connectionist Temporal Classification (CTC) is applied for text recognition (Shi, Bai, and Yao 2016; Liu et al. 2016; He et al.

*Equal Contribution.

¹https://github.com/JarveeLee/SynthText_Chinese_version

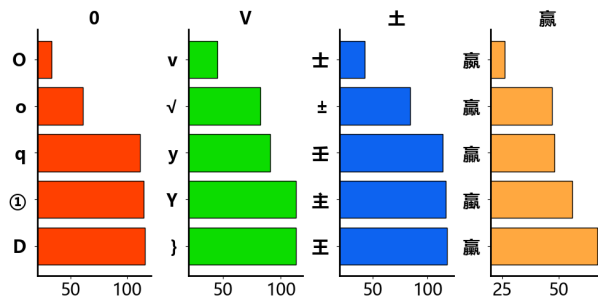


Figure 1: Hamming distances between characters. The vocabulary size is over 20,000. Several characters are selected and their top 5 nearest characters are shown. Note that the LSH code for each character contains 512 bits.

2015; Wang and Hu 2017) to obtain the sequence of characters corresponding to the text image without character-level segmentation. (Shi, Bai, and Yao 2016) integrates Recurrent Neural Network (RNN) with CTC to extract rich contextual information and make the decoding parallel and fast. However, these CTC-based methods are insufficient to deal with irregular text.

Recently, the attention mechanism, which is proposed to tackle machine translation in (Bahdanau, Cho, and Bengio 2014), is widely used to handle text recognition. For RNN-attention-based models (Lee and Osindero 2016; Cheng et al. 2017; Ghosh, Valveny, and Bagdanov 2017), CNN and RNN are used as the encoder to extract contextual feature and another RNN combined with attention mechanism is employed as the decoder to align and decode character at each time step. A 2D attention mechanism, which can learn to select individual character features in the 2D space for decoding character, is proposed by (Li et al. 2019). (Wang et al. 2020) proposes a convolutional alignment module with UNet-style network architecture to address the misalignment issue. Inspired by the Transformer (Vaswani et al. 2017), (Yang et al. 2020; Lu et al. 2019) employ several transformer units to model the dependence among the sequence of output characters and align the visual features with the output character at each time-step.

Many state-of-the-art works adopt heavy models. For instance, Master (Lu et al. 2019) uses ResNet31 (He et al.

2016) and several transformer units. It is over 220MB. Obviously, its impractical to directly deploy these models on mobile system due to the immense storage overhead and computational cost. PaddleOCR² provides a super lightweight CRNN (Shi, Bai, and Yao 2016) using MobileNetV3 (Howard et al. 2019) to reduce model size from 31.8MB to 4.5MB.

The softmax regression layer used in these methods, contains a projection matrix W with size $d \times L$, where d is the dimension of the character-level feature and L is the length of vocabulary list. To reduce the storage cost, we need a small L and small d . However, small d hurts the model performance and small L limits its application in many scenarios, such as Chinese and multi-language character recognition. For example, the storage cost of matrix W is 39.1MB when the vocabulary size is 20,000 and d is 512. More over, in (Li et al. 2019; Lu et al. 2019), a matrix with similar size is used in the embedding layer to encode the output character.

To address these issues, we propose a lightweight model, named Hamming OCR, to support scene text recognition with a large scale vocabulary. Hamming OCR is composed of four components: feature encoder, transformer decoder, Hamming embedding, and Hamming classifier, as shown in Figure 2.

In the Hamming classifier, we use LSH (Gionis et al. 1999) to map the output of a pre-trained model’s feature layer to Hamming space. A majority voting mechanism is used to generate the representation code for each character. Due to the natural of LSH code, visual similar characters will be mapped codes with small Hamming distance, as shown in Figure 1. In the training stage, we employ a Hinge-loss to learn the optimal projection matrix for the target code.

Compare with the traditional one-hot encoding used in softmax, LSH code is multi-hot and more efficient when the vocabulary size is large. For example, given a vocabulary with 20,000 characters and a feature layer of 512-dimension, the storage cost of the Hamming classifier is 1.22MB, which is 32 times smaller than softmax regression. Moreover, the LSH code is directly used in the output embedding, and the number of model parameters is further reduced.

Like (Lu et al. 2019; Yang et al. 2020; Yu et al. 2020), we solely use transformer units to align and decode characters. To reduce the number of parameters, we remove the feed-forward component of the transformer unit and propose cross-layer parameter sharing for different transformer units. To deploy the model on mobile devices, we balance performance and model size, MobileNetV2 (Sandler et al. 2018) is chosen as the feature encoder.

In summary, our contributions are summarized as follows:

- We present a method to generate the LSH code to map each character to Hamming space. In this space, visual similar characters will have small Hamming distance.
- We propose a novel Hamming classifier trained by Hinge-loss, which predicts output character using multi-hot LSH

encoding instead of one-hot encoding. Using this strategy, the model’s storage cost is significantly reduced when the vocabulary is large.

- The LSH code is directly used in the output embedding module. It further reduces the computational cost and model size.
- We also simplify the transformer decoder architecture by removing the feed-forward module and cross-layer parameter sharing.
- Hamming OCR delivers competitive results on several scene text datasets, which is based on self-attention mechanism. More importantly, it can handle a large scale vocabulary and its size is very small.

Related Work

Given an input image I , the goal of scene text recognition is to produce a sequence (y_1, y_2, \dots, y_T) , where $y_t \in \{1, 2, \dots, L\}$ is the character indicator, L is the length of a predefined vocabulary list V .

Generally, attention-based text recognition models (Li et al. 2019; Lu et al. 2019; Yu et al. 2020) have higher accuracy on irregular text datasets, which have an encoder-decoder architecture. Here, we mainly focus on attention-based models and divide a model into four basic components according to their role, including feature encoder, decoder, output embedding, and classifier.

The first component is feature encoder which maps the input text image to a representation. In order to extract high-level visual features, ResNet is regard as the most popular CNN. For instance, (Hu et al. 2020; Yu et al. 2020; Baek et al. 2019) adopt ResNet50 as the feature encoder’s backbone, and (Lu et al. 2019; Ghosh, Valveny, and Bagdanov 2017) use ResNet31 as the feature encoder. Meanwhile, many other types of ResNet (Li et al. 2019; Shi et al. 2018) also are utilized. To enlarge the feature context, RNN over feature sequence is adopted (Shi et al. 2018; Shi, Bai, and Yao 2016). However, ResNet is inconvenient to deploy on the mobile system due to its storage requirement.

Decoder is the second component, which is used for sequence modeling. (Li et al. 2019) adopts a 2-layer RNN with a 2D attention mechanism to decode the holistic feature into a sequence of characters. With transformer achieving success in natural language processing, (Lu et al. 2019; Yang et al. 2020; Yu et al. 2020) utilize self-attention module as decoder to learn character dependencies. They directly use the Transformer decoder which is composed of a masked self-attention mechanism to model relations between different characters of the output sequence, an attention module aligning character-level features from encoder with the output characters, and a feed-forward layer. However, the storage consuming of transformer decoder cannot be ignored. For instance, a typical feed-forward layer contains two projection matrices with size 2048×512 .

Output embedding is widely used for sequence model. For text recognition, it encodes the output character of the previous time step as input for the decoder to decode the next character. Usually, learned embeddings (Lu et al. 2019;

²<https://github.com/PaddlePaddle/PaddleOCR>

Vaswani et al. 2017) are employed to convert the input characters to vectors of dimension d . If we have L characters for embedding, the size of the weight matrix of output embedding is $L \times d$. As the number of characters increases, the memory consumption of output embedding is unbearable for mobile devices.

One of the most common classification approaches is softmax regression. Most text recognition methods directly use softmax regression to map the character-level features into probabilities over the vocabulary V . In the following subsection, we introduce softmax regression.

Softmax Regression for Classification

Text recognition is a sequence prediction problem. At each time step, decoder extracts a character-level feature vector by use of attention mechanism. Then the character-level feature vector is mapped into the probability distribution over V as

$$\Pr(y|h, W) = \frac{\exp(w_y^T h)}{\sum_{j=1}^L \exp(w_j^T h)}, \quad (1)$$

where $h \in \mathcal{F}$ denotes the character-level feature generated by decoder at each time step. \mathcal{F} represents a d -dimensional character-level feature space. $w_j \in \mathbb{R}^d$ denotes the j -th column of the weight $W \in \mathbb{R}^{d \times L}$. Then, classification decision is given by

$$\hat{y} = \arg \max_{j \in \{1, 2, \dots, L\}} \Pr(y = j|h, W). \quad (2)$$

In the training process, to maximize the probability of the ground-truth sequence at each time step, hence, the cross-entropy loss $-\log(\Pr(y|h, W))$ is employed.

Hamming OCR Model

As shown in Figure 2(b), the Hamming OCR model contains four main components, feature encoder, transformer decoder, Hamming embedding, and Hamming classifier. In this section, we will first introduce the idea of LSH codebook for Hamming OCR model, then we will give the detail of each model components.

LSH Codebook for Hamming OCR Model

Different from the traditional OCR models, we use multi-hot codes as the training target, and the model output is also directly used in the output embedding layer. According to the experimental result, which will be shown later in Table 3, the design of the multi-hot codebook isn't trivial. Randomly generated codebook will hurt the model performance significantly. Therefore the Hamming OCR model cannot be trained directly without the LSH codebook.

To address this issue, we use an auxiliary model which replace the Hamming classifier with softmax regression, and Hamming embedding with the traditional embedding technique, which is shown in Figure 2 (a). This model can be trained end to end directly.

Using this model, any input text image is mapped into a sequence of character-level feature vectors $\{h_t \in \mathcal{F}\}_{t=1}^T$ for

classification. Since the classifier isn't dependent on time-step t , we omit the time-step index and define $h_{i,j} \in \mathcal{F}$ to represent the j -th feature of i -th character class. Then we use LSH algorithm to project each feature vector $h_{i,j}$ to a d' -bits binary vector $b_{i,j}$ as follow

$$b_{i,j}^k = \text{sgn}(\psi_k^T h_{i,j}), \quad (3)$$

where $b_{i,j}^k$ is the k -th bit of the vector $b_{i,j}$, ψ_k is the k -th vector of the random projection matrix $\Psi \in \mathbb{R}^{d \times d'}$.

Since the softmax loss has the tendency to force the feature vectors from the same class to be close in the feature space, after the LSH mapping, the codes from the same character class will be close in the Hamming space as well. Based on this assumption, a majority vote algorithm is used to generate representation code for each character class.

$$\eta_i^k = I\left(\sum_j b_{i,j}^k > n_i/2\right), \quad (4)$$

where η_i^k is the k -th bit of the LSH code η_i for the i -th character class, n_i is the number of feature vectors in the i -th class, and $I(\cdot)$ is the indicator function which has the value 1 when the input is true and has the value 0 when the input is false. Finally, we get the codebook $\eta = [\eta_1, \eta_2, \dots, \eta_L]$ corresponding to the vocabulary V .

Theoretically, there is a chance that two character class has the same representation vector. However, when $d > 256$, the chance of such conflict is small. Actually, even for the similar characters, The Hamming distance between the corresponding codes is not small. For example, visually, the character "0" looks like "o". Their LSH codes generated by our method also are similar to each other. From Figure 1, the Hamming distance between "0" and "o" is much smaller than the others, which is 33. It means that the edit distance between their LSH code is 33.

Hamming Classifier

For each input vector $h_{i,j}$, the Hamming classifier will output a binary vector of d' bits, using the equation:

$$b_{i,j}^k = \text{sgn}(w_k^T h_{i,j}), \quad (5)$$

where $b_{i,j}^k$ is the k -th bit of the output binary vector $b_{i,j}$, w_k is the k -th column of the projection matrix W used in the Hamming classifier. We hope that the output code $b_{i,j}$ should be close to the target code η_i in the Hamming space.

To achieve this goal, we propose to use the Hinge-loss (Cortes and Vapnik 1995) to train the whole model and find optimal W . The loss is defined as follow:

$$\mathcal{L} = \sum_{i,j,k} \{\max\{0, \theta - w_k^T h_{i,j}\} \eta_i^k + \max\{0, \theta + w_k^T h_{i,j}\} (1 - \eta_i^k)\}, \quad (6)$$

where θ is the margin, w_k is the k -th project vector of W , η_i^k is the k -th bit of the target code for the i -th class.

The Hamming classifier will map a feature vector into a point in a multi-dimension space. In each dimension of the space, the points from the same class will distribute in the

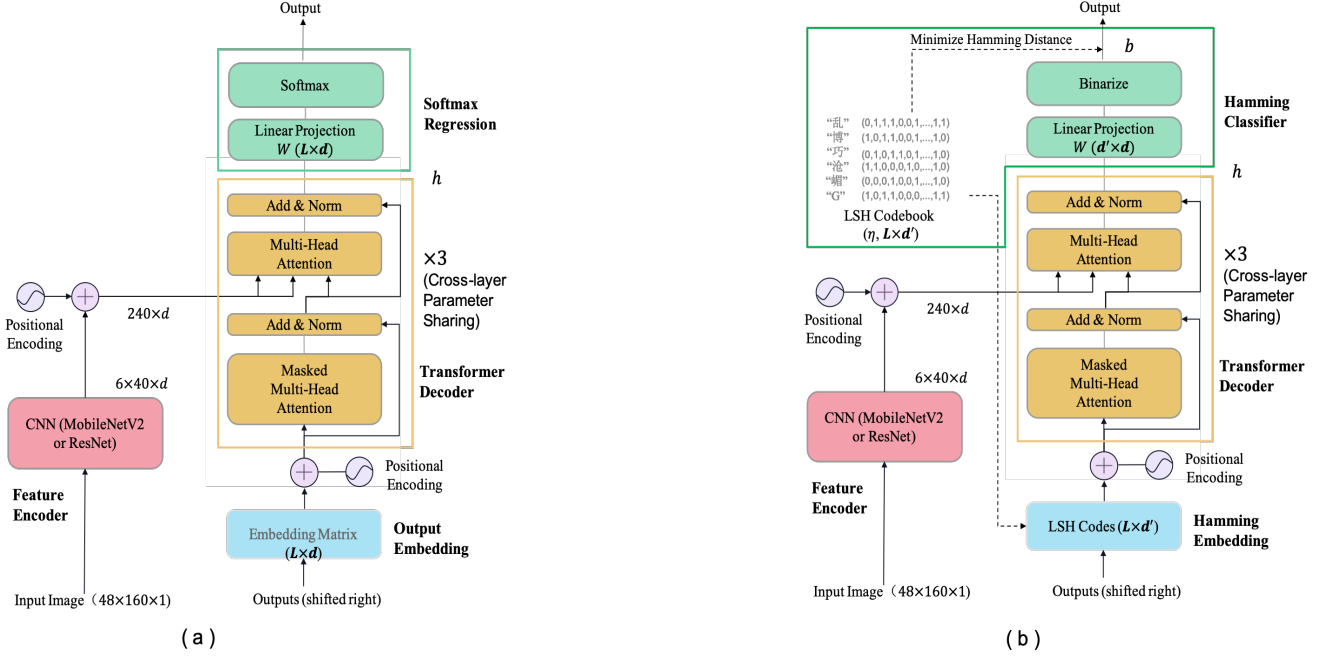


Figure 2: (a) The model architecture of the auxiliary model. (b) The architecture of Hamming OCR model.

same side of the axis. Due to the nature of Hinge-loss, these points are also be pushed away from the origin. It will reduce the chance of encoding error.

In the inference stage, we use the Equation (5) to calculate the binary vector b for each feature vector h . However, due to the possible classifier error, the binary code b may not be exist in the codebook η . To address this issue, we use:

$$\hat{y} = \arg \min_{j \in \{1, 2, \dots, L\}} \text{HammingDistance}(b, \eta_j), \quad (7)$$

to generate the prediction \hat{y} .

Hamming Embedding

This component is used to encode the output character. Traditional methods try to learn a d -dimensional vector as embedding for each character. As the number of characters increase, the memory consumption of output embedding also increases proportionally. When there is a large vocabulary, the storage cost of the output embedding is heavy. To address this issue, we use the output codes as embedding of output characters as shown in Figure 2.

Feature Encoder

We choose the backbone of Master (Lu et al. 2019) as our network's backbone, which integrates ResNet31 with GCNet (Cao et al. 2019). Considering the model size and time consuming, for mobile applications, a lightweight MobileNetV2, which is presented in Appendix A, is used as our feature encoder.

Transformer Decoder

Attention mechanism can align relevant visual features to the corresponding output character, which aggregates information from the entire input sequence. Inspired by Transformer, the decoder of Transformer is applied to model sequence prediction in text recognition. A standard decoder of Transformer is composed of a stack of N identical layers, each of which has three sub-layers. The first sub-layer is a masked self-attention network, the second one is a self-attention network and the third one is a feed-forward network. $Y^\ell \in \mathbb{R}^{T \times d}$ that is embedding of the output sequence is denoted as the input tensor of the ℓ -th layer, then, these three sub-modules can be written as the following equations:

$$Y^\ell = \cup_{k=1}^H \text{Att}(Y_Q^\ell W_{k,\ell}^Q, Y_K^\ell W_{k,\ell}^K, Y_V^\ell W_{k,\ell}^V) \cdot W_\ell^O \quad (8a)$$

$$Y^\ell = \cup_{k=1}^H \text{Att}(Y^\ell U_{k,\ell}^Q, X U_{k,\ell}^K, X U_{k,\ell}^V) \cdot U_\ell^O \quad (8b)$$

$$Y^\ell = \text{ReLU}(Y^\ell W_1^{\text{FF}} + b_1^{\text{FF}}) W_2^{\text{FF}} + b_2^{\text{FF}} \quad (8c)$$

where $\text{Att}(\cdot)$ is scaled dot-product attention (Vaswani et al. 2017), H is the number of heads and $\cup_{k=1}^H$ denotes a concatenated operator. In Equation (8a), $Y_Q^\ell, Y_K^\ell, Y_V^\ell$ are masked Y^ℓ to prevent a given position from incorporating information about future output positions. X in Equation (8b) is extracted by the feature encoder. Note that residual connections and layer normalization are used for each sub-layer, which don't show in Equation (8a), (8b) and (8c).

For the ℓ -th layer, $\{W_{k,\ell}^Q, W_{k,\ell}^K, W_{k,\ell}^V\}_{k=1}^H \in \mathbb{R}^{d \times \frac{d}{H}}$, and $W_\ell^O \in \mathbb{R}^{d \times d}$ are parameters corresponding to masked multi-head self-attention sub-layer. $\{U_{k,\ell}^Q, U_{k,\ell}^K, U_{k,\ell}^V\}_{k=1}^H \in$

$\mathbb{R}^{d \times \frac{d}{H}}$, and $U_\ell^O \in \mathbb{R}^{d \times d}$ are parameters of multi-head self-attention modules. $W_1^{FF} \in \mathbb{R}^{d \times 2048}$, $W_2^{FF} \in \mathbb{R}^{2048 \times d}$, and $b_1^{FF} \in \mathbb{R}^{2048}$, $b_2^{FF} \in \mathbb{R}^d$ are parameters of feed-forward sub-layer. There are many parameters for one layer of transformer decoder.

Removing the feed-forward network and cross-layer parameter sharing techniques are employed in our transformer decoder to reduce the storage requirement, which stacks three transformer decoder layers. From Equation (8c), we find that the main function of a feed-forward network with two linear transformations is to learn a projection. However, in Equation (8a) and (8b), each of them contains a projection matrix (W_ℓ^O, U_ℓ^O) which has similar function with feed-forward network. More importantly, feed-forward network has many parameters. So, we remove the feed-forward network (Equation (8c)) in each layer of transformer decoder. For one layer of our transformer decoder, it contains two sub-layers. The first sub-layer is a masked self-attention network and another one is a self-attention network as is shown in Figure 2. Like (Lan et al. 2019), cross-layer parameter sharing technique is used for all the three layers of our transformer decoder. That means, the parameters in Equation (8a) and (8b) keep the same values for different layers.

Table 1: Model size of Hamming OCR under different settings.

	Hamming OCR						
	×	✓	✓	✓	✓	✓	✓
MobileNetV2	×	✓					
Hamming Classifier	×		✓				
Hamming Embedding	×			✓			
No Feed-Forward	×				✓		
Cross-layer Parameter Sharing	×					✓	
Half-Precision Float (FP16)	×						✓
Model Size	305.8Mb	55.6Mb	36.7Mb	16.6Mb	10.6Mb	6.6Mb	3.9Mb

Parameter Analysis

In this subsection, we analyze the storage requirement of different models under different settings. Our baseline model has similar with (Lu et al. 2019), which uses a ResNet31 with GCNet as CNN’s backbone and three-layer transformer decoder. We choose a vocabulary with 20,948 characters. Then, we compute that the baseline model requires 305.8Mb storage resource. When MobileNetV2 is used to replace ResNet31, the model size sharply reduces to 55.6Mb. Different from the baseline model, Hamming OCR adopts many techniques to reduce the model size including Hamming Classifier, Hamming Embedding, removing feed-forward network of transformer decoder, and cross-layer parameter sharing. Table 1 shows the model size for each model. Our MobileNetV2-based Hamming OCR only costs 6.6Mb. Additionally, when we use 16-bit floating point to represent the weights of Hamming OCR, the most lightweight Hamming OCR is 3.9Mb.

Experiments

We conduct extensive experiments to verify the effectiveness of our Hamming OCR. First, several public standard datasets are employed. However, these public datasets only contain English words and the number of characters to be recognized

is relatively small. In order to further validate the capability of Hamming OCR, a dataset named as GBK21K is newly generated.

Datasets

IIT 5K-Words (IIT5K) (Mishra, Alahari, and Jawahar 2012) contains 3,000 cropped scene text images for testing. **Street View Text (SVT)** (Wang, Babenko, and Belongie 2011) consists of 257 training images and 647 testing images, which is collected from Google Street Image.

SVT-Perspective (SVTP) (Quy Phan et al. 2013) consists of 645 cropped images. Many images have perspective distortions.

CUTE80 (CUTE) contains 288 text patches cropped from natural scene images for curved text recognition.

MJSynth (MJ) (Jaderberg et al. 2014) consists of 9 millions image instances, which is randomly generated based on 90k English words.

GBK21K is generated with the engine in (Gupta, Vedaldi, and Zisserman 2016), which includes 3 million text patches for training and 30k cropped images for testing. The text of each cropped image is generated by randomly selecting several characters from a vocabulary collected in advance. This vocabulary is a subset of the GBK Chinese characters³ and contains 20,948 characters including Chinese, English and numeric characters. The dataset is challenging due to low-resolution, clustered background, different fonts, and various illumination. Figure 3 illustrates several cropped images and ground-truth texts.



Figure 3: Examples of text in GBK21K. Several cropped images and corresponding ground truth texts are shown.

Training Strategy

The training of Hamming OCR includes two stages. In the first stage, we train an auxiliary model which uses ordinary output embedding and softmax regression. Cross entropy loss is used in this stage. With the trained model, we generate the codebook for all characters. In the second stage, we replace the output embedding with the Hamming embedding and the softmax regression with the Hamming classifier. The parameters of the backbone and transformer decoder are initially loaded from the model trained in the first stage. We retrain the model using Hinge-loss.

We implement our Hamming OCR with PyTorch and run all experiments on NVIDIA Tesla V100 GPUs with 16GB memory. The batch size on each GPU is 160, with 8 GPUs in total. All input images are padded and resized to 48×160 .

³[https://en.wikipedia.org/wiki/GBK_\(character_encoding\)](https://en.wikipedia.org/wiki/GBK_(character_encoding))

For standard benchmarks, without any data augmentation, we directly use synthetic data MJSynth (7.2M) as our training data. There are 62 characters to be recognized. For the GBK21K dataset, we generate 3M cropped images for training and evaluate the performance on 30K text images. GBK21k is used for Chinese text recognition and contains 20,948 symbol classes. We adopt the Adam optimizer, and the following hyper-parameters are used: the initial learning rate of 0.001 and the decay rate of 0.5.

Recognition Performance Evaluation

The recognition accuracies of different methods on five datasets, including regular (IIIT5K, SVT), irregular (SVTP, CUTE) and a Chinese text (GBK21K), are shown in Table 2. In Hamming OCR model, four techniques are used including Hamming classifier, Hamming embedding, removing feed-forward network and cross-layer parameter sharing. To compare the effect of different techniques, we design three models based on the Master model by: replacing the softmax regression with Hamming classifier, namely HC; replacing the softmax regression and output embedding with Hamming classifier and Hamming embedding respectively, namely HC+HE; and employing removing feed-forward network and cross-layer parameter sharing technique, namely NoFFN+PS.

Firstly, we analyze the performance of different methods on the four standard benchmarks. Compared with previous methods with the same training data (MJ), Hamming OCR achieves competitive results. Especially, HC+HE has the similar performance as Master in most situations, which verifies the effectiveness of the proposed Hamming classifier and Hamming embedding. When we use removing feed-forward network and cross-layer parameter sharing techniques in transformer decoder module, the results of NoFFN+PS are slightly lower than Master. Due to the lightweight CNN backbone, the results of Hamming OCR (MobileNetV2) significantly decrease. However, Hamming OCR (MobileNetV2) consistently outperforms PaddleOCR in comparison with the same training data. For instance, the accuracy of Hamming OCR model on IIIT5K is higher than the larger PaddleOCR model by one percentage, while its model size is smaller. Aster has outstanding results on irregular datasets due to its rectification module.

Secondly, On the GBK21K dataset, compared with Master, Hamming OCR not only obtains competitive performance but also sharply reduces the storage cost. The results show that Hamming OCR can handle such challenging Chinese recognition task. For the lightweight models, our Hamming OCR (MobileNetV2) outperforms PaddleOCR. Hamming OCR (MobileNetV2) includes a backbone of 2.3Mb, a simplified transformer decoder of 2.5Mb, a projection matrix of 0.5Mb and a codebook of 1.3Mb, while the PaddleOCR (MobileNetV3, large) includes a backbone of 3.0Mb, an LSTM decoder of 0.9Mb and a softmax classifier of 7.8Mb. It can be seen that softmax regression take a large portion of the storage cost of PaddleOCR.

In Hamming OCR, the projection matrix Ψ used to generate the LSH codebook is randomly initialized. When we directly evaluate the performance of Hamming OCR with

this initial projection matrix, its results are 50.9% on IIIT5K, 48.5% on SVT, 32.7% on SVTP, 32.3% on CUTE. Therefore, we confirm that retraining the model with the Hinge-loss is very vital.

Ablation Study

Factorized Embedding Vs LSH Code. From a practical perspective, Chinese or multi-language text recognition usually require the length of the vocabulary list L to be large, then increasing L increases the size of the embedding matrix ($d \times L$) from output embedding and the projection matrix ($d \times L$) from softmax regression. As ALBERT (Lan et al. 2019), we use a factorized embedding technique, which decomposes a matrix into two smaller matrices, to reduce the parameters. We take the linear transformation $W \in \mathbb{R}^{d \times L}$ of softmax regression as an example. It can be decomposed into $W_1 \in \mathbb{R}^{d \times p}$ and $W_2 \in \mathbb{R}^{p \times L}$. By using this decomposition, we reduce the parameters W from $\mathcal{O}(d \times L)$ to $\mathcal{O}(d \times p + p \times L)$. This parameter reduction is significant when $d \gg p$. On the other hand, we present the LSH code can significantly reduce the parameters in classifier and output embedding modules. Thus, in this part, we take the experiments on GBK21K to evaluate the performance of factorized embedding technique and our Hamming classifier.

From Figure 4, we can see that as the value of p increases, the recognition accuracy of the model based on factorized embedding technique is also increasing. Compared with factorized embedding technique, Hamming OCR performs better and its size is smaller.

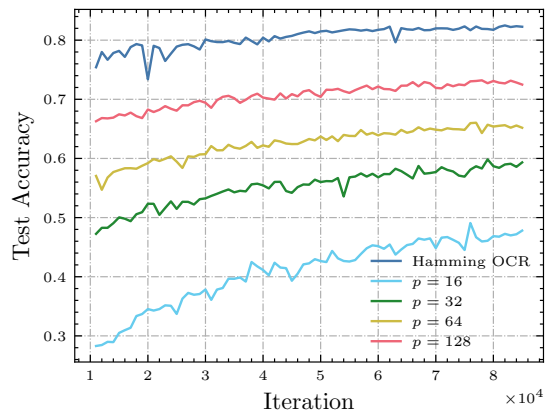


Figure 4: Performance comparison on GBK21K with different training steps. The performance of factorized embedding technique with $p = 16, 32, 64, 128$ are demonstrated.

Random Code Vs LSH Code. In our Hamming OCR, we obtain LSH code by linear projection and thresholding. To verify the effectiveness of LSH code, we compare its performance with a random code, which is simply generated by a random method. To generate each element of the random code for a character, we randomly choose 0 or 1 with equal probability. To be fair, we adopt HC as the baseline model. Table 3 illustrates the recognition results on datasets. We can see that the performance of random code on the

Table 2: Performance and model size (Mb) comparison on several public benchmarks and a Chinese text dataset. Master* represents the model trained on an union of MJSynth (MJ), SynthText (Gupta, Vedaldi, and Zisserman 2016) (ST) and SynthAdd (Gupta, Vedaldi, and Zisserman 2016) (SA). PaddleOCR† and PaddleOCR‡ represent the officially supplied model and the model trained by ourselves with the official code respectively. “HC” and “HE” mean Hamming classifier and Hamming embedding are used respectively, “NoFFN” and “PS” are corresponding to removing feed-forward network and cross-layer parameter sharing techniques for transformer decoder. The index “Ratio (%)” represents the ratio of model size of Hamming classifier and output embedding in the whole model.

Methods	Public Benchmarks						Chinese Text Recognition		
	Training Data	Mode Size	IIT5K	SVT	SVTP	CUTE	Mode Size	Ratio (%)	GBK21K
RARE (Shi et al. 2016)	MJ	—	81.9	81.9	71.8	59.2	—	—	—
Yang et al. (Yang et al. 2017)	MJ	—	—	—	75.8	69.3	—	—	—
R ² AM (Lee and Osindero 2016)	MJ	—	78.4	80.7	—	—	—	—	—
CRNN (Shi, Bai, and Yao 2016)	MJ	31.8	78.2	80.8	—	—	72.7	56.3	—
CRNN (VGG) (Shi et al. 2018)	MJ	—	81.2	82.7	—	—	—	—	—
ASTER-A (Shi et al. 2018)	MJ	—	81.7	80.2	73.2	63.9	—	—	—
ASTER-B (Shi et al. 2018)	MJ	80.4	83.2	81.6	75.4	67.4	161.9	49.7	—
PaddleOCR‡ (MobileNetV3, large)	MJ+ST	—	83.7	84.1	71	62.2	—	—	—
ASTER (Shi et al. 2018)	MJ+ST	—	93.4	89.5	78.5	79.5	—	—	—
SAR (Li et al. 2019)	MJ+ST+SA	—	91.5	84.5	76.4	83.3	—	—	—
Master* (Lu et al. 2019)	MJ+ST+SA	223.9	95.0	91.8	84.5	87.5	305.9	13.4	—
Master (ResNet31)	MJ	223.9	85.4	85.3	74.1	69.8	305.9	13.4	82.3
HC (ResNet31)	MJ	224.7	85.7	85.6	74.1	69.1	267.0	16.3	82.4
HC+HE (ResNet31)	MJ	224.6	85.9	85.6	74.6	68.4	226.9	1.4	82.5
NoFFN+PS (ResNet31)	MJ	184.0	84.8	83.9	73.2	69.8	266.1	30.9	82.1
Hamming OCR (ResNet31)	MJ	184.8	85.0	84.5	73.0	69.1	187.1	1.2	82.8
PaddleOCR† (MobileNetV3, small)	MJ	2.7	79.5	79.8	63.7	52.4	9.4	82.7	48.3
PaddleOCR† (MobileNetV3, large)	MJ	5.3	81.6	80.7	68.2	58.7	11.7	66.4	66.5
Hamming OCR (MobileNetV2)	MJ	4.6	82.6	83.3	68.8	61.1	6.6	27.1	71.2

four standard benchmarks is competitive. For example, the recognition accuracy of LSH code is 85.6% while random code can reach 84.5% on the SVT dataset. However, for the GBK21K dataset, model with random code does not converge at all and can’t recognize any text image correctly. As we know, the lexicon of SVT is very small, the random code can represent each character very well. However, there are over 20,000 characters in GBK21K, it’s possible that the representation ability of random code is insufficient. Different from random code, LSH code can reach 82.4% recognition rate on GBK21K dataset.

Table 3: Performance comparison of baseline model with LSH code and random code on GBK21K. * means the model does not converge.

Methods	IIT5K	SVT	SVTP	CUTE	GBK21K
Random Code	81.53	84.54	73.18	68.06	0.00*
LSH Code	85.70	85.63	74.11	69.10	82.41

Influence of The Length of LSH Code. Table 4 demonstrates the variation of recognition rate along with the length of LSH code. Obviously, LSH code with 512-dimension performs very well. When the length of LSH code is less than 512, the performance of Hamming OCR has declined. As the length of LSH code is larger than 512, the performance almost saturates. However, its negative impact is that the model size obviously becomes larger.

Table 4: Performance with different lengths of LSH code on GBK21K.

Length (LSH Code)	256	512	1024	2048
GBK21K (accuracy)	81.86	82.39	82.26	82.31

Conclusion

In this paper, we present a lightweight and effective Hamming OCR method for scene text recognition. Most scene text recognition approaches adopt learnable output embedding and softmax regression for decoding the output characters and classification. Each of them has a parameter matrix, the size of which depends on the number of characters. when we need deploy a model with a large scale lexicon on mobile devices, these two matrices are encumbrances due to their massive storage requirements. Therefore, we present a method to generate a codebook for all characters and develop a Hamming classifier for classification. We further use the LSH code of each character as its embedding. As we know, this work is the first attempt to use LSH code as the representation vector of each class for classification and embedding. To reduce the parameters of a standard decoder of transformer, we introduce a simplified transformer decoder by removing the feed-forward network and using cross-layer parameter sharing technique. We combine Hamming classifier, Hamming embedding, and simplified transformer decoder into Hamming OCR. Hamming OCR achieve competitive results on on several standard benchmarks and one our own dataset.

References

- Baek, J.; Kim, G.; Lee, J.; Park, S.; Han, D.; Yun, S.; Oh, S. J.; and Lee, H. 2019. What is wrong with scene text recognition model comparisons? dataset and model analysis. In *Proceedings of the IEEE International Conference on Computer Vision*, 4715–4723.
- Bahdanau, D.; Cho, K.; and Bengio, Y. 2014. Neural machine translation by jointly learning to align and translate. *arXiv preprint arXiv:1409.0473*.
- Cao, Y.; Xu, J.; Lin, S.; Wei, F.; and Hu, H. 2019. Gnet: Non-local networks meet squeeze-excitation networks and beyond. In *Proceedings of the IEEE International Conference on Computer Vision Workshops*, 0–0.
- Chen, X.; Jin, L.; Zhu, Y.; Luo, C.; and Wang, T. 2020. Text Recognition in the Wild: A Survey. *arXiv preprint arXiv:2005.03492*.
- Cheng, Z.; Bai, F.; Xu, Y.; Zheng, G.; Pu, S.; and Zhou, S. 2017. Focusing attention: Towards accurate text recognition in natural images. In *Proceedings of the IEEE international conference on computer vision*, 5076–5084.
- Cheng, Z.; Xu, Y.; Bai, F.; Niu, Y.; Pu, S.; and Zhou, S. 2018. Aon: Towards arbitrarily-oriented text recognition. In *Proceedings of the IEEE Conference on Computer Vision and Pattern Recognition*, 5571–5579.
- Cortes, C.; and Vapnik, V. 1995. Support-vector networks. *Machine learning* 20(3): 273–297.
- Ghosh, S. K.; Valveny, E.; and Bagdanov, A. D. 2017. Visual attention models for scene text recognition. In *2017 14th IAPR International Conference on Document Analysis and Recognition (ICDAR)*, volume 1, 943–948. IEEE.
- Gionis, A.; Indyk, P.; Motwani, R.; et al. 1999. Similarity search in high dimensions via hashing. In *Vldb*, volume 99, 518–529.
- Gupta, A.; Vedaldi, A.; and Zisserman, A. 2016. Synthetic data for text localisation in natural images. In *Proceedings of the IEEE conference on computer vision and pattern recognition*, 2315–2324.
- He, K.; Zhang, X.; Ren, S.; and Sun, J. 2016. Deep residual learning for image recognition. In *Proceedings of the IEEE conference on computer vision and pattern recognition*, 770–778.
- He, P.; Huang, W.; Qiao, Y.; Loy, C. C.; and Tang, X. 2015. Reading scene text in deep convolutional sequences. *arXiv preprint arXiv:1506.04395*.
- Howard, A.; Sandler, M.; Chu, G.; Chen, L.-C.; Chen, B.; Tan, M.; Wang, W.; Zhu, Y.; Pang, R.; Vasudevan, V.; et al. 2019. Searching for mobilenetv3. In *Proceedings of the IEEE International Conference on Computer Vision*, 1314–1324.
- Hu, W.; Cai, X.; Hou, J.; Yi, S.; and Lin, Z. 2020. GTC: Guided Training of CTC towards Efficient and Accurate Scene Text Recognition. In *AAAI*, 11005–11012.
- Jaderberg, M.; Simonyan, K.; Vedaldi, A.; and Zisserman, A. 2014. Synthetic data and artificial neural networks for natural scene text recognition. *arXiv preprint arXiv:1406.2227*.
- Lan, Z.; Chen, M.; Goodman, S.; Gimpel, K.; Sharma, P.; and Soricut, R. 2019. Albert: A lite bert for self-supervised learning of language representations. *arXiv preprint arXiv:1909.11942*.
- Lee, C.-Y.; and Osindero, S. 2016. Recursive recurrent nets with attention modeling for ocr in the wild. In *Proceedings of the IEEE Conference on Computer Vision and Pattern Recognition*, 2231–2239.
- Li, H.; Wang, P.; Shen, C.; and Zhang, G. 2019. Show, attend and read: A simple and strong baseline for irregular text recognition. In *Proceedings of the AAAI Conference on Artificial Intelligence*, volume 33, 8610–8617.
- Liu, W.; Chen, C.; and Wong, K.-Y. K. 2018. Char-Net: A Character-Aware Neural Network for Distorted Scene Text Recognition. In *AAAI*, volume 1, 4.
- Liu, W.; Chen, C.; Wong, K.-Y. K.; Su, Z.; and Han, J. 2016. STAR-Net: A SpaTial Attention Residue Network for Scene Text Recognition. In *BMVC*, volume 2, 7.
- Lu, N.; Yu, W.; Qi, X.; Chen, Y.; Gong, P.; and Xiao, R. 2019. Master: Multi-aspect non-local network for scene text recognition. *arXiv preprint arXiv:1910.02562*.
- Mishra, A.; Alahari, K.; and Jawahar, C. 2012. Top-down and bottom-up cues for scene text recognition. In *2012 IEEE Conference on Computer Vision and Pattern Recognition*, 2687–2694. IEEE.
- Quy Phan, T.; Shivakumara, P.; Tian, S.; and Lim Tan, C. 2013. Recognizing text with perspective distortion in natural scenes. In *Proceedings of the IEEE International Conference on Computer Vision*, 569–576.
- Sandler, M.; Howard, A.; Zhu, M.; Zhmoginov, A.; and Chen, L.-C. 2018. Mobilenetv2: Inverted residuals and linear bottlenecks. In *Proceedings of the IEEE conference on computer vision and pattern recognition*, 4510–4520.
- Shi, B.; Bai, X.; and Yao, C. 2016. An end-to-end trainable neural network for image-based sequence recognition and its application to scene text recognition. *IEEE transactions on pattern analysis and machine intelligence* 39(11): 2298–2304.
- Shi, B.; Wang, X.; Lyu, P.; Yao, C.; and Bai, X. 2016. Robust scene text recognition with automatic rectification. In *Proceedings of the IEEE conference on computer vision and pattern recognition*, 4168–4176.
- Shi, B.; Yang, M.; Wang, X.; Lyu, P.; Yao, C.; and Bai, X. 2018. Aster: An attentional scene text recognizer with flexible rectification. *IEEE transactions on pattern analysis and machine intelligence* 41(9): 2035–2048.
- Vaswani, A.; Shazeer, N.; Parmar, N.; Uszkoreit, J.; Jones, L.; Gomez, A. N.; Kaiser, Ł.; and Polosukhin, I. 2017. Attention is all you need. In *Advances in neural information processing systems*, 5998–6008.

Wang, J.; and Hu, X. 2017. Gated recurrent convolution neural network for ocr. In *Advances in Neural Information Processing Systems*, 335–344.

Wang, K.; Babenko, B.; and Belongie, S. 2011. End-to-end scene text recognition. In *2011 International Conference on Computer Vision*, 1457–1464. IEEE.

Wang, T.; Zhu, Y.; Jin, L.; Luo, C.; Chen, X.; Wu, Y.; Wang, Q.; and Cai, M. 2020. Decoupled Attention Network for Text Recognition. In *AAAI*, 12216–12224.

Yang, L.; Wang, P.; Li, H.; Li, Z.; and Zhang, Y. 2020. A Holistic Representation Guided Attention Network for Scene Text Recognition. *Neurocomputing*.

Yang, X.; He, D.; Zhou, Z.; Kifer, D.; and Giles, C. L. 2017. Learning to Read Irregular Text with Attention Mechanisms. In *IJCAI*, volume 1, 3.

Yu, D.; Li, X.; Zhang, C.; Liu, T.; Han, J.; Liu, J.; and Ding, E. 2020. Towards accurate scene text recognition with semantic reasoning networks. In *Proceedings of the IEEE/CVF Conference on Computer Vision and Pattern Recognition*, 12113–12122.